Geophysical Journal International

Geophys. J. Int. (2015) **202,** 914–919 doi: 10.1093/gji/ggv194
GJI Seismology

Spatial-temporal variation of low-frequency earthquake bursts near Parkfield, California

Chunquan Wu,[1] Robert Guyer,[2] David Shelly,[3] Daniel Trugman,[4] William Frank,[5] Joan Gomberg[6] and Paul Johnson[1]

[1]*Geophysics Group, Los Alamos National Laboratory, Los Alamos, NM* 87545, *USA. E-mail: chunquanwu@gmail.com*
[2]*Physics Department, University of Nevada, Reno, NV* 89557, *USA*
[3]*US Geological Survey, Menlo Park, CA* 94025, *USA*
[4]*Scripps Institution of Oceanography, UC San Diego, La Jolla, CA* 92093, *USA*
[5]*Laboratory of Seismology, IPGP, Paris, France*
[6]*US Geological Survey, Seattle, WA* 98195, *USA*

Accepted 2015 May 6. Received 2015 May 5; in original form 2015 January 28

SUMMARY

Tectonic tremor (TT) and low-frequency earthquakes (LFEs) have been found in the deeper crust of various tectonic environments globally in the last decade. The spatial-temporal behaviour of LFEs provides insight into deep fault zone processes. In this study, we examine recurrence times from a 12-yr catalogue of 88 LFE families with ∼730 000 LFEs in the vicinity of the Parkfield section of the San Andreas Fault (SAF) in central California. We apply an automatic burst detection algorithm to the LFE recurrence times to identify the clustering behaviour of LFEs (LFE bursts) in each family. We find that the burst behaviours in the northern and southern LFE groups differ. Generally, the northern group has longer burst duration but fewer LFEs per burst, while the southern group has shorter burst duration but more LFEs per burst. The southern group LFE bursts are generally more correlated than the northern group, suggesting more coherent deep fault slip and relatively simpler deep fault structure beneath the locked section of SAF. We also found that the 2004 Parkfield earthquake clearly increased the number of LFEs per burst and average burst duration for both the northern and the southern groups, with a relatively larger effect on the northern group. This could be due to the weakness of northern part of the fault, or the northwesterly rupture direction of the Parkfield earthquake.

Key words: Seismicity and tectonics; Continental margins: transform; North America.

1 INTRODUCTION

Tectonic tremors (TTs) are weak, continuous seismic signals without clear impulsive P- and S-phase arrivals. TT was first observed in southwestern Japan (Obara 2002) and later found along other major plate boundaries, primarily subduction zones (e.g. Peng & Gomberg 2010, and references therein). TT signals are generally thought to be associated with slow slip on fault segments deeper than the regular seismogenic zone (e.g. Rogers & Dragert 2003), and are suggested to be largely comprised by swarms of low-frequency earthquakes (LFEs), which are generated by slip on small on-fault asperities (Ide *et al.* 2007; Shelly *et al.* 2007; Frank *et al.* 2013, 2015a; Royer & Bostock 2014). It has been proposed that TT and LFE patterns may provide information about fault slip below the seismogenic zone, and thus potentially future earthquake occurrence (Shelly 2009, 2010a; Rubinstein *et al.* 2010).

TTs and LFEs have been observed along both the northwest creeping and southeast locked sections of the San Andreas fault (SAF) in central California (Nadeau & Dolenc 2005; Nadeau & Guilhem 2009; Shelly *et al.* 2009; Shelly & Hardebeck 2010). On the other hand, geodetic observations of the deep slow slip events responsible for the TT and LFE signals near Parkfield have not been reported so far, presumably due to relatively small geodetic moment release (e.g. Smith & Gomberg 2009). Hence, investigation of the spatial-temporal patterns of TTs and LFEs is the only way to infer deep fault slip information beneath the upper crustal seismogenic zone (Guilhem & Nadeau 2012; Frank *et al.* 2015b). Shelly (2010a) examined the spatial migration pattern of the SAF tremors, and found multiple migration episodes at the rate of ∼15–80 km hr^{-1}. These results suggested that the deep SAF is a generally a through-going structure, but the distinct tremor rate changes of different tremor sources along the SAF after the 2004 *M*6.0

Parkfield earthquake indicated heterogeneous fault friction properties. Previous studies also found increased TT and LFE activities during the Parkfield earthquake followed by gradual recovery (Nadeau & Guilhem 2009; Shelly & Johnson 2011; Guilhem & Nadeau 2012; Wu *et al.* 2013).

Previous studies mostly focused on investigation of individual LFE source location and recurrence patterns, which primarily provide information on individual small asperities rather than the aseismic slip on the surrounding fault interface that causes the LFE activities. In this paper, rather than examining the occurrence pattern of individual LFEs, we study the clustering of LFEs using a new automatic detection method to identify LFE 'bursts', which are periods in which a single LFE source radiates repeatedly at an elevated rate. We use this method to investigate the spatial-temporal correlation of different LFE sources, in the hope to better understand the deep fault slip behaviour, and to constrain the scale of heterogeneity beneath different sections of SAF, from the locked Cholame section southeast of Parkfield that last ruptured in the 1857 M7.9 Fort Tejon earthquake (Sieh 1978) to the northwest creeping section between Parkfield and San Benito (Fig. 1). We then compare the influences of the 2004 Parkfield earthquake on the northern and southern LFE burst characteristics. Finally, we discuss possible physical explanations of the observations, and their implications on the deep SAF structure and friction properties.

2 DATA AND ANALYSIS PROCEDURE

We utilize an LFE catalogue from 2001 to 2012, in which groups of repeated similar LFEs are put into an LFE family (Shelly & Hardebeck 2010). LFE families are located using P- and S-arrival times measured from stacked seismic waveforms, and repeated occurrences of similar LFEs are identified by cross-correlation of the LFE family template waveforms with the continuous seismic recordings at multiple High-Resolution Seismic Network (HRSN) stations (Shelly *et al.* 2009). The locations of the 88 LFE families (with a total of ∼730 000 LFEs) used in this study are shown in Fig. 1. The depths range from ∼16 to ∼30 km and their estimated moment magnitudes are generally <0.5 (e.g. Nadeau & Dolenc 2005).

We develop an automatic burst detection algorithm and apply it to the LFE catalogue to identify temporal clusters of repeated radiated seismic energy from a single LFE source (Fig. 2). We first compute the LFE recurrence times (time between successive LFEs in the same family, R_t in Fig. 2) from the LFE catalogue. We then estimate the reference LFE recurrence time (T_R) for each LFE family by computing the arithmetic average of all the recurrence times within the family, and use four times the reference recurrence time as the threshold to find LFE bursts. We group all the consecutive LFEs that occur within a duration of $4T_R$ into an LFE burst; a burst ends when the time to the next LFE exceeds $4T_R$. We set a burst size threshold of 50 (i.e. require at least 50 LFEs within a burst) to ensure elevated LFE activity during bursts. We have tested the size of recurrence time threshold from $2T_R$ to $10T_R$, and varying the burst size threshold from 30 to 100 LFEs. The results show no substantial difference in the general patterns of detected LFE bursts. Fig. S1 illustrates the robustness of our algorithm to detect elevated LFE activities, and shows that the detected LFE bursts provide a more straightforward way to compare the temporal clustering behaviour of two LFE families than using the individual LFE recurrence times (e.g. Shelly 2010b; Wu *et al.* 2013). We then examine the spatial correlation of the LFE bursts between all the LFE family pairs. We obtain the one-bit correlation coefficient by defining the period during an LFE burst as one and the period with no burst as zero, and then computing the correlation coefficient between a pair of LFE families. Finally, we compare the burst patterns and responses to the 2004 Parkfield earthquake of the northern and southern LFE families.

3 RESULTS

After applying the automatic burst detection algorithm to the LFE catalogue, we detected a total of ∼6700 LFE bursts, including ∼2800 bursts in the northern families, and ∼3900 bursts in the southern families. The distributions of number of bursts, total number of LFEs in bursts, cumulative, minimum, maximum, and average duration of bursts for all the families are shown in Fig. S2. The number of bursts in each family varies from less than 10 to ∼100, and there are generally more LFEs in bursts in the southern families than in the northern families. The correlation between number of LFEs in bursts and the number of bursts is high for the northern families and the southern families with less than 40 bursts, but not for the southern families with more than 40 bursts (Fig. S3), indicating those southern families with relatively more bursts also have higher LFE rates within bursts. Fig. 3 shows the overall spatial-temporal pattern of LFE bursts for all the families aligned along the SAF. We did not observe any progressive variation of LFE burst behaviour from north to south. We observe similar temporal patterns of bursts from about −40 to −15 km to the south of Parkfield, and from about 10 to 18 km, 22 to 30 km and 40 to 44 km to the north of Parkfield (Fig. 3). The families from −40 to −15 km and 22 to 30 km along SAF have more bursts than the other families, and the families from –30 to –20 km and 22 to 30 km along SAF have higher LFE rates within bursts than the other families (Fig. 3). We also compared the burst patterns of LFE families at similar SAF locations but different depths (Fig. S4), and our results suggest that the shallower families generally have more bursts than the deeper families.

To constrain the spatial extent of the deep fault slips that generate simultaneous LFE bursts at different sources, we compute the one-bit correlation coefficient of LFE burst time between all LFE family pairs and identify the LFE families with similar burst patterns (Fig. 4). The correlation coefficients for the family pairs within the southern and northern groups is generally much higher than the correlation coefficients between family pairs with one family from each of the southern and northern groups. The highest correlation coefficient is ∼0.9 between two adjacent families at −26 km to the south of Parkfield, and the lowest correlation coefficients are close to 0 between some north-south family pairs. The average correlation coefficient between all the family pairs in the southern group (0.35) is higher than the average value for the northern group (0.26).

Fig. 3 also shows significantly increased LFE burst activities after the 2004 Parkfield earthquake. After the Parkfield earthquake, some LFE bursts with very long duration occur in multiple families of both the northern and southern groups. We hypothesized that the Parkfield earthquake caused a strong increase in the aseismic slip rate, which would be manifest as increased LFE activities and longer bursts. To test this hypothesis, we compute average number of LFEs per burst and average burst duration at each time point for the northern and southern groups, respectively (Fig. 5). Fig. 5(a) shows a clear increase in the number of LFEs per burst for both the northern and southern groups after the Parkfield earthquake, and the increase in the northern group is much larger than that in

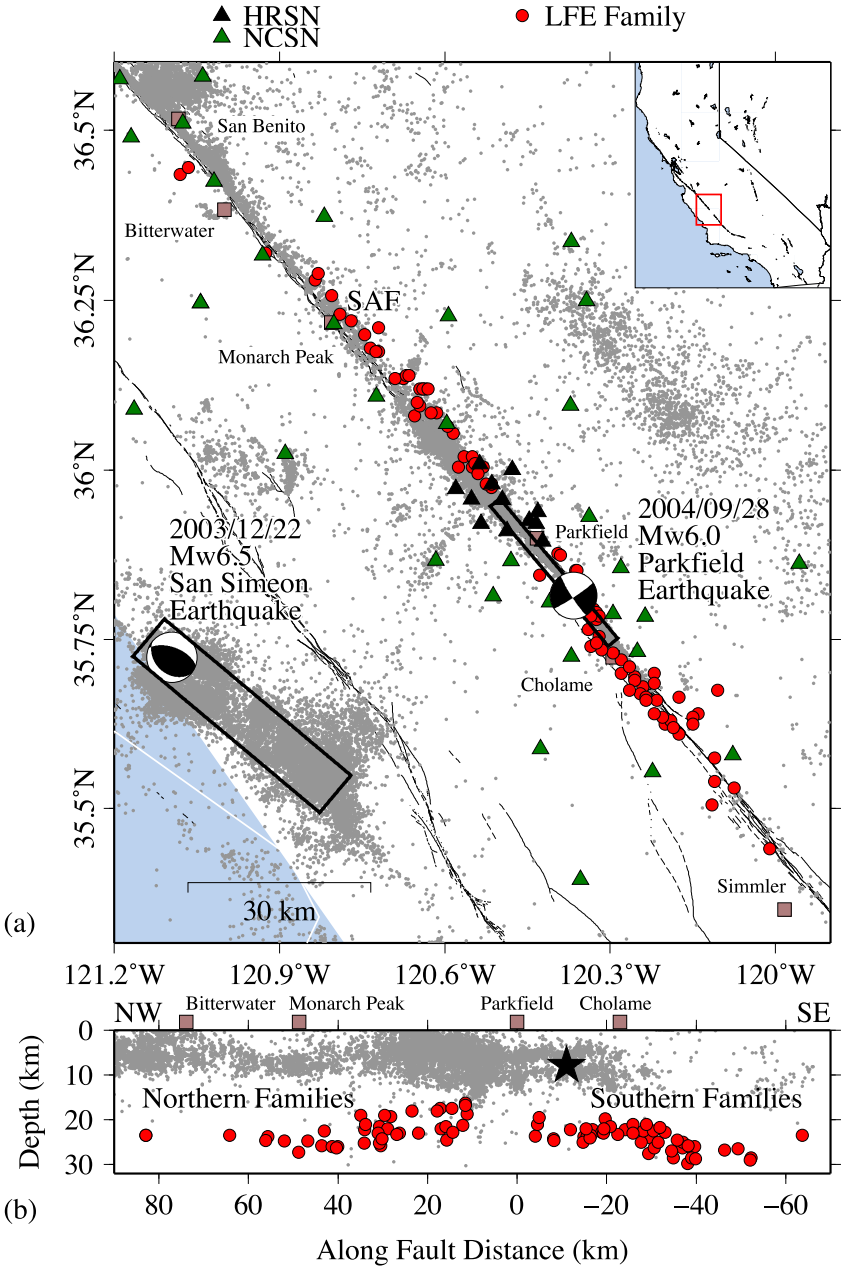

Figure 1. (a) Map of the study region of central California. The solid red circles show the locations of the 88 low-frequency earthquake (LFE) families used in this study. The epicentres of the 2003 M_w 6.5 San Simeon and the 2004 M_w 6.0 Parkfield earthquakes are indicated by the moment tensor solutions, with the black boxes showing the rupture zones (Chen *et al.* 2004; Bennington *et al.* 2011). The black triangles show the locations of the HRSN stations, and the green triangles show the locations of the NCSN stations. The small grey dots show the background seismicity from 2000 to 2012 listed in the Northern California Earthquake Data Center (NCEDC) catalogue. The black lines indicate active faults and the brown squares indicate the geographical locations. The inset is a map of California with the red box showing the region plotted in the main map. (b) Cross-sectional view along the San Andreas fault (SAF). The black star indicates the 2004 Parkfield earthquake hypocentre. The solid red circles show the depths and along SAF location of the 88 LFE families. The other symbols are the same as in panel (a).

the southern group. Similarly, Fig. 5(b) shows clear increases in the average burst duration after the Parkfield earthquake, with a much larger increase in the northern group. The changes after the 2003 San Simeon earthquake are generally not clear, but there is a small increase in the average number of LFEs per burst in both groups 1.5 months before the San Simeon earthquake, coinciding with noise reductions at some HRSN stations. We also observe a significant decrease in the LFE burst recurrence times for some of the families after the Parkfield earthquake (e.g. Fig. S5).

4 DISCUSSION

TT or groups of LFEs are generally presumed to be caused by transient aseismic slip in the deep fault (e.g. Rogers & Dragert 2003). By investigating the spatial-temporal correlation of LFE bursts along SAF, we hope to better constrain the scales of variations in the deep fault slip and the conditions that give rise to these variations. Previous studies have documented burst behaviour of LFEs in Japan, central California and Mexico (Shelly *et al.* 2007;

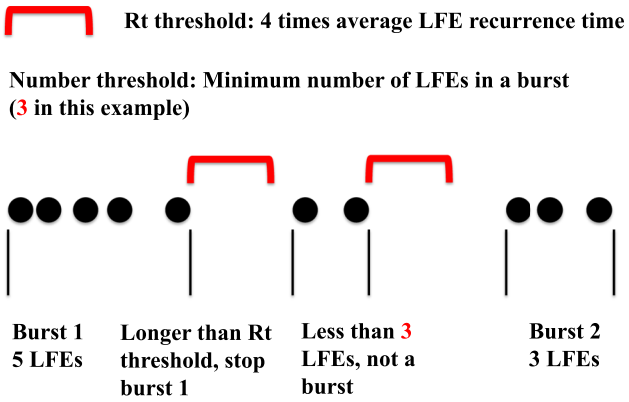

Figure 2. Schematic illustration of the automatic burst detection algorithm.

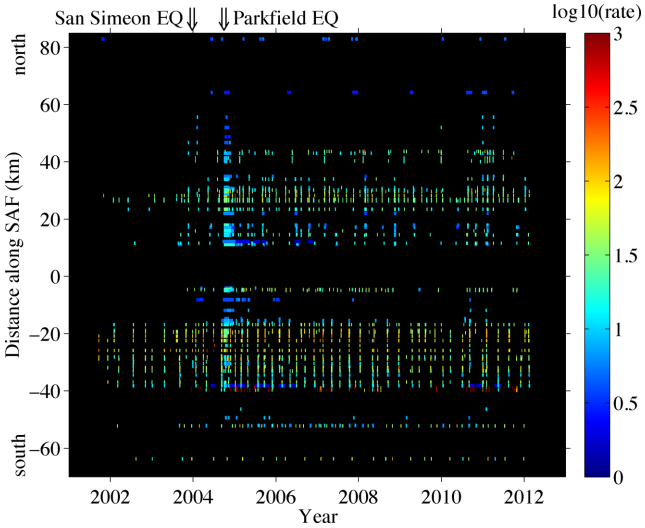

Figure 3. The timing of LFE bursts for all the 88 LFE families aligned by the distance along the SAF. The *X*-axis is calendar year and the *Y*-axis is distance along SAF. The width of colour-coded rectangles show the starting and ending times of LFE bursts, with the colour showing the LFE rate per day in logarithmic scale. The two arrows at the top of the figure mark the timings of the 2003 San Simeon and the 2004 Parkfield earthquakes, respectively.

Shelly 2010b; Frank *et al.* 2013, 2014). Shelly & Johnson (2011) examined the patterns for LFE sources at different depths in central California, and found that the shallower sources are generally more clustered in time than the deeper sources. Guilhem & Nadeau (2012) compared the occurrence patterns of TTs and LFEs at Parkfield and suggested that the dependence of LFE patterns on along-fault location is more significant than the depth dependence.

Here we investigated the LFE burst behaviour in central California quantitatively, and observed clear spatial coherence in the LFE burst patterns. The automatic burst detection method provides a more objective way to quantify the clustered activities of LFEs (Fig. S1), which also enables quantification of the correlation between LFE bursts from different sources (Figs 3 and 4). The strong correlation of LFE bursts within the southern groups found in this study (Figs 3 and 4) suggests coherent slip behaviour beneath the Cholame section of SAF, and that the deep fault structure is likely to be relatively simple (Wesnousky 2006). On the other hand, we observe three different groups of LFE burst patterns to the north of Parkfield (Fig. 3), suggesting variation in slip behaviour among these groups, which could be indicative of more variable fault zone

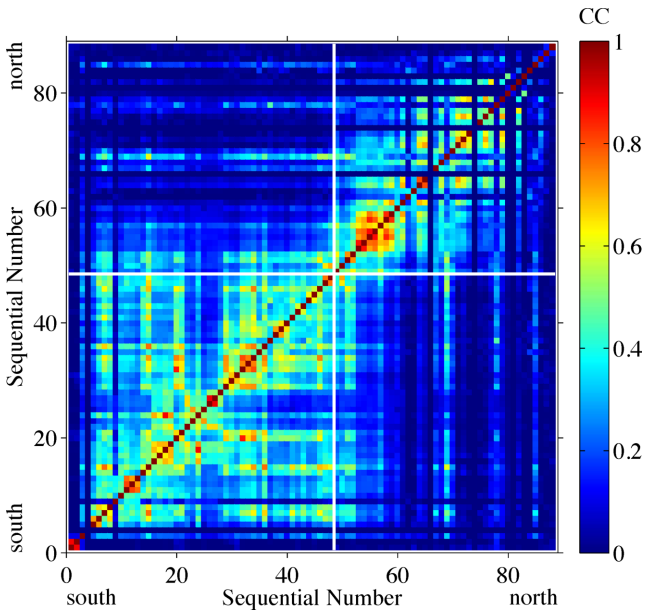

Figure 4. Plot showing the correlation coefficient (CC) value of the LFE bursts for all the LFE family pairs. The LFE families are sorted by position from south to north along SAF in both *X*- and *Y*-axes. The horizontal and vertical white lines mark the boundaries between the southern and northern families.

structure, frictional properties and permeability (Yamashita 2013). Investigation of the burst patterns for LFE families at similar along-fault locations but different depths shows that the shallower families have more LFE bursts than the deeper families (Fig. S4), suggesting a transition from stick-slip at the shallower sources to stable sliding at the deep sources (Shelly & Johnson 2011). However, the LFE sources close to Parkfield are generally shallower than those sources further north and south (Fig. 1), and there are uncertainties of LFE source depth due to the LFE detection algorithm (Shelly & Hardebeck 2010; Guilhem & Nadeau 2012), so it is difficult to completely separate the along-fault dependence with the depth dependence of LFE burst patterns. Possible explanations for the abrupt changes in elastic properties of deep SAF include multiple fault strands at depth (Field 2007; Nadeau & Guilhem 2009), weakening with increasing depth and temperature (Obara *et al.* 2010), and high thermal gradient of SAF (Shelly & Johnson 2011).

Temporal changes in LFE and tremor activities after the 2003 San Simeon and 2004 Parkfield earthquakes have been documented in some previous studies (Nadeau & Guilhem 2009; Shelly & Johnson 2011; Guilhem & Nadeau 2012; Wu *et al.* 2013). Shelly & Johnson (2011) showed that the San Simeon earthquake had small and mixed effects on different LFE sources, while the Parkfield earthquake had large and universally promoting effects on all the LFE sources. In this study, we examine the influence of these two earthquakes on the LFE burst characteristics instead of individual LFEs to investigate the temporal variation in deep fault slip. Temporal changes in LFE burst patterns are subtle after the San Simeon earthquake, but are striking after the Parkfield earthquake (Fig. 5). When we average the results in both groups, the small and mixed effects caused by the San Simeon earthquake are likely cancelled out, so the changes are not obvious in Fig. 5. The number of LFEs per burst and the average burst duration in both groups increase after the Parkfield earthquake (Fig. 5), indicating extended period of deep fault slip along different sections of SAF. This is likely due to the large positive Coulomb stress on both groups caused by the

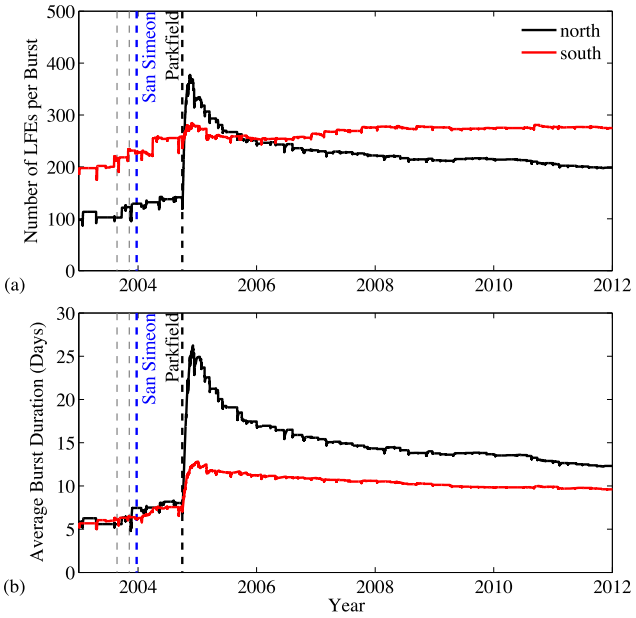

Figure 5. (a) The black and red curves show the temporal changes in the number of LFEs per burst (cumulative numbers of LFEs divided by cumulative number of bursts at each time point) for the northern and southern LFE families, respectively. The vertical blue and black dashed lines show the timings of the 2003 San Simeon and the 2004 Parkfield earthquakes, respectively. The vertical grey dashed lines show the timings of the HRSN gain changes. (b) Similar plot as (a) for the temporal changes in the average burst duration.

Parkfield earthquake and its afterslip (Shelly & Johnson 2011). Fig. 5 also shows that the northern group has longer average burst duration, while the southern group has more LFEs per burst, suggesting that the northern group bursts are generally less clustered than the southern group bursts. In addition, the increases of both number of LFEs per burst and burst duration in the northern group is much larger than that in the southern group after the Parkfield earthquake (Fig. 5). Both observations suggest that the friction strength of the deep SAF beneath the creeping section of SAF north of Parkfield is likely to be weaker than that beneath the locked Cholame section, mirroring the changing friction strength in the upper crust from the creeping section to the locked section of SAF (Lockner *et al.* 2011; Shelly & Johnson 2011). Other possible explanations of the larger effects on the northern group is the dynamic effects and focusing due to the northwestern rupture direction of the Parkfield earthquake (Bakun *et al.* 2005), and potential differing effects on various types of bursts from the perturbation of the Parkfield earthquake, which will be investigated in a follow-up synthetic modelling study.

5 CONCLUSION

We develop an automatic LFE burst detection method and apply it to the 12-yr LFE catalogue in Parkfield (Shelly & Hardebeck 2010). We found that the northern group of LFE sources generally has longer burst duration but fewer LFEs within bursts, while the southern group has shorter burst duration but more LFEs within bursts. The southern group LFE bursts are generally more correlated than the northern group, suggesting more coherent deep fault slip and relatively simpler deep fault structure beneath the locked section of SAF. The 2004 Parkfield earthquake increased the number of LFEs per burst and burst durations for both the northern and southern groups, with a relatively larger effect on the northern group. Our observations indicate that the frictional strength of the deep SAF northwest of Parkfield is likely to be weaker than that at the Cholame section. This study, together with other recent studies (e.g. Frank *et al.* 2015a), suggest that the LFE burst method is an effective new approach to characterize deep fault slip.

ACKNOWLEDGEMENTS

This research was supported by Institutional Support at Los Alamos National Lab (CW, RG, DT and PJ), USGS (DS and JG), and IPGP (WF). We thank Andrew Delorey and Eric Daub for helpful discussions. We thank Abhijit Ghosh and Aaron Wech for their useful comments and suggestions. The HRSN is operated by UC Berkeley. Data were obtained through the Northern California Earthquake Data Center (NCEDC) and Southern California Earthquake Data Center (SCEDC, doi:10.7909/C3WD3xH1).

REFERENCES

Bakun, W. *et al.*, 2005. Implications for prediction and hazard assessment from the 2004 Parkfield earthquake, *Nature,* **437,** 969–974.

Bennington, N., Thurber, C., Feigl, K.L. & Murray-Moraleda, J., 2011. Aftershock distribution as a constraint on the geodetic model of coseismic slip for the 2004 Parkfield earthquake, *Pure appl. Geophys.,* **168,** 1553–1565.

Chen, J., Larson, K.M., Tan, Y., Hudnut, K.W. & Choi, K., 2004. Slip history of the 2003 San Simeon earthquake constrained by combining 1-Hz GPS, strong motion, and teleseismic data, *Geophys. Res. Lett.,* **31,** doi:10.1029/2004GL020448.

Field, E.H., 2007. A summary of previous working groups on California earthquake probabilities, *Bull. seism. Soc. Am.,* **97,** 1033–1053.

Frank, W., Shapiro, N., Husker, A., Kostoglodov, V., Bhat, H. & Campillo, M., 2015a. Along-fault pore-pressure evolution during a slow-slip event in Guerrero, Mexico, *Earth planet. Sci. Lett.,* **413,** 135–143.

Frank, W.B., Shapiro, N.M., Husker, A.L., Kostoglodov, V., Romanenko, A. & Campillo, M., 2014. Using systematically characterized low-frequency earthquakes as a fault probe in Guerrero, Mexico, *J. geophys. Res.: Solid Earth,* **119,** 7686–7700.

Frank, W.B., Shapiro, N.M., Kostoglodov, V., Husker, A.L., Campillo, M., Payero, J.S. & Prieto, G.A., 2013. Low-frequency earthquakes in the Mexican Sweet Spot, *Geophys. Res. Lett.,* **40,** 2661–2666.

Frank, W.B., Radiguet, M., Rousset, B., Shapiro, N.M., Husker, A.L., Kostoglodov, V., Cotte, N. & Campillo, M., 2015b. Uncovering the geodetic signature of silent slip through repeating earthquakes, *Geophys. Res. Lett.,* **42,** doi:10.1002/2015GL063685.

Guilhem, A. & Nadeau, R.M., 2012. Episodic tremors and deep slow-slip events in Central California, *Earth planet. Sci. Lett.,* **357,** 1–10.

Ide, S., Shelly, D.R. & Beroza, G.C., 2007. Mechanism of deep low frequency earthquakes: Further evidence that deep non-volcanic tremor is generated by shear slip on the plate interface, *Geophys. Res. Lett.,* **34,** L03308, doi:10.1029/2006GL028890.

Lockner, D.A., Morrow, C., Moore, D. & Hickman, S., 2011. Low strength of deep San Andreas fault gouge from SAFOD core, *Nature,* **472,** 82–85.

Nadeau, R.M. & Dolenc, D., 2005. Nonvolcanic tremors deep beneath the San Andreas fault, *Science,* **307,** 389–389.

Nadeau, R.M. & Guilhem, A., 2009. Nonvolcanic tremor evolution and the San Simeon and Parkfield, California, earthquakes, *Science,* **325,** 191–193.

Obara, K., 2002. Nonvolcanic deep tremor associated with subduction in southwest Japan, *Science,* **296,** 1679–1681.

Obara, K., Tanaka, S., Maeda, T. & Matsuzawa, T., 2010. Depth-dependent activity of non-volcanic tremor in southwest Japan, *Geophys. Res. Lett.,* **37,** doi:10.1029/2010GL043679.

Peng, Z. & Gomberg, J., 2010. An integrated perspective of the continuum between earthquakes and slow-slip phenomena, *Nat. Geosci.,* **3,** 599–607.
Rogers, G. & Dragert, H., 2003. Episodic tremor and slip on the Cascadia subduction zone: The chatter of silent slip, *Science,* **300,** 1942–1943.
Royer, A. & Bostock, M., 2014. A comparative study of low frequency earthquake templates in northern Cascadia, *Earth planet. Sci. Lett.,* **402,** 247–256.
Rubinstein, J.L., Shelly, D.R. & Ellsworth, W.L., 2010. Non-volcanic tremor: A window into the roots of fault zones, *New Front. Integrat. Solid Earth Sci.,* 287–314.
Shelly, D.R., 2009. Possible deep fault slip preceding the 2004 Parkfield earthquake, inferred from detailed observations of tectonic tremor, *Geophys. Res. Lett.,* **36,** L17318, doi:10.1029/2009GL039589.
Shelly, D.R., 2010a. Migrating tremors illuminate complex deformation beneath the seismogenic San Andreas fault, *Nature,* **463,** 648–652.
Shelly, D.R., 2010b. Periodic, chaotic, and doubled earthquake recurrence intervals on the deep San Andreas Fault, *Science,* **328,** 1385–1388.
Shelly, D.R. & Hardebeck, J.L., 2010. Precise tremor source locations and amplitude variations along the lower-crustal central San Andreas Fault, *Geophys. Res. Lett.,* **37,** L14301, doi:10.1029/2010GL043672.
Shelly, D.R. & Johnson, K.M., 2011. Tremor reveals stress shadowing, deep postseismic creep, and depth-dependent slip recurrence on the lower-crustal San Andreas fault near Parkfield, *Geophys. Res. Lett.,* **38,** L13312, doi:10.1029/2011GL047863.
Shelly, D.R., Beroza, G.C. & Ide, S., 2007. Non-volcanic tremor and low-frequency earthquake swarms, *Nature,* **446,** 305–307.
Shelly, D.R., Ellsworth, W.L., Ryberg, T., Haberland, C., Fuis, G.S., Murphy, J., Nadeau, R.M. & Bürgmann, R., 2009. Precise location of San Andreas Fault tremors near Cholame, California using seismometer clusters: slip on the deep extension of the fault?, *Geophys. Res. Lett.,* **36,** L01303, doi:10.1029/2008GL036367.
Sieh, K.E., 1978. Central California foreshocks of the great 1857 earthquake, *Bull. seism. Soc. Am.,* **68,** 1731–1749.
Smith, E.F. & Gomberg, J., 2009. A search in strainmeter data for slow slip associated with triggered and ambient tremor near Parkfield, California, *J. geophys. Res.,* **114,** B00A14, doi:10.1029/2008JB006040.
Wesnousky, S.G., 2006. Predicting the endpoints of earthquake ruptures, *Nature,* **444,** 358–360.
Wu, C., Shelly, D.R., Gomberg, J., Peng, Z. & Johnson, P., 2013. Long-term changes of earthquake inter-event times and low-frequency earthquake recurrence in central California, *Earth planet. Sci. Lett.,* **368,** 144–150.
Yamashita, T., 2013. Generation of slow slip coupled with tremor due to fluid flow along a fault, *Geophys. J. Int.,* **193**(1), 375–393.

SUPPORTING INFORMATION

Additional Supporting Information may be found in the online version of this paper:

Figure S1. Illustration of the period of elevated LFE activities captured by the automatic burst detection algorithm. The *X*-axis is the calendar year and the *Y*-axis is the LFE recurrence time (R_t) in logarithmic scale. The black circles show individual LFEs in (a) LFE family 32 and (b) LFE family 25, which are ∼2.3 km apart in the south group. The vertical red lines indicate the detected LFE bursts, with the width of each line showing the duration of the burst. The horizontal blue dashed line shows the recurrence time threshold to define LFE bursts.

Figure S2. (a) Number of LFE bursts for each of the 88 LFE families, sorted from south to north along the *X*-axis by their projected positions along the San Andreas Fault (SAF). The vertical red dashed line indicates the boundary between the southern and northern families. (b) Similar plot as (a) for number of LFEs within bursts. (c) Similar plot as (a) for the total duration of bursts in days. (d–f) Similar plots as (a) for the minimum, maximum and average duration of bursts in days.

Figure S3. (a) Number of LFEs within bursts versus number of bursts for all the northern families. The red line shows first order least squares fitting of the data. The correlation coefficient between the observed data (black circles) and fitted curve (red line) is marked at the bottom right corner. (b) Similar plot as (a) for all the southern families. The red and blue lines show first order least-squares fitting of the data in the <40 and >40 ranges, respectively.

Figure S4. Comparison of the LFE burst patterns for families at similar along SAF locations but different depths. The *X*-axis is the calendar year and the *Y*-axis is the LFE recurrence time (R_t) in logarithmic scale. The black circles show individual LFEs in (a) LFE family 42 at the depth of 16.3 km and (b) LFE family 41 at the depth of 24.5 km, which are ∼4.2 km apart in the north group, and in (c) LFE family 60 at the depth of 22 km and (d) LFE family 39 at the depth of 25 km, which are ∼0.7 km apart in the south group. The vertical red lines indicate the detected LFE bursts, with the width of each line showing the duration of the burst. The horizontal blue dashed line shows the recurrence time threshold to define LFE bursts.

Figure S5. Examples of the temporal changes in LFE burst recurrence times for two families: (a) LFE family 26 and (b) LFE family 42. The *X*-axis is the calendar year and the *Y*-axis is the LFE burst recurrence time. The blue and black vertical dashed lines show the occurrence times of the San Simeon and Parkfield earthquakes, respectively. The red dashed curve show the least squares fitting of the burst recurrence times after the Parkfield earthquake.
(http://gji.oxfordjournals.org/lookup/suppl/doi:10.1093/gji/ggv194/-/DC1)

Please note: Oxford University Press is not responsible for the content or functionality of any supporting materials supplied by the authors. Any queries (other than missing material) should be directed to the corresponding author for the paper.